Acta Crystallographica Section F
Structural Biology and Crystallization Communications
ISSN 1744-3091

Crystallization and preliminary X-ray diffraction analysis of the complex of Kunitz-type tamarind trypsin inhibitor and porcine pancreatic trypsin

Sakshi Tomar, Dipak N. Patil, Manali Datta, Satya Tapas, Preeti, Anshul Chaudhary, Ashwani K. Sharma, Shailly Tomar* and Pravindra Kumar*

Department of Biotechnology, Indian Institute of Technology, Roorkee, Roorkee 247667, India

Correspondence e-mail: shailfbt@iitr.ernet.in, kumarfbs@iitr.ernet.in

Received 12 September 2009
Accepted 12 October 2009

The complex of *Tamarindus indica* Kunitz-type trypsin inhibitor and porcine trypsin has been crystallized by the sitting-drop vapour-diffusion method using ammonium acetate as precipitant and sodium acetate as buffer. The homogeneity of complex formation was checked by size-exclusion chromatography and further confirmed by reducing SDS–PAGE. The crystals diffracted to 2.0 Å resolution and belonged to the tetragonal space group $P4_1$, with unit-cell parameters $a = b = 57.1$, $c = 120.1$ Å. Preliminary X-ray diffraction analysis indicated the presence of one unit of inhibitor–trypsin complex per asymmetric unit, with a solvent content of 45%.

1. Introduction

Proteases are proteinaceous enzymes that catalyze the hydrolytic cleavage of the peptide bond. These enzymes play a vital role in nonspecific digestion of intracellular and extracellular proteins and are specifically required for the proteolytic cleavage of inactive precursors, the activation of zymogens, the processing of hormones and neuropeptides, the activation of receptors, protein translocation through membranes *etc.* (Neurath, 1984). One class of proteases are the serine proteases (EC 3.4.21), which are thus classified owing to the presence of a serine residue in their active site. These proteolytic enzymes are actively involved in various physiological processes such as the coagulation of blood, complement system activation, fertilization, the hypersensitive response, microsporogenesis, cell proliferation and differentiation and signal transduction *via* protein degradation/processing (Neurath, 1986; Antão & Malcata, 2005). With proteases being involved in so many important functions, the significance of the antagonist becomes equally crucial. Moderation of activity is performed by a class of ubiquitous moieties called protease inhibitors (PIs). Various classes of inhibitors have been studied extensively as they have the potential to act as therapeutic agents. Among these, serine protease inhibitors have been the most studied and have been isolated from various sources including Leguminosae seeds (Macedo *et al.*, 2000; Macedo & Xavier-Filho, 1992; Mello *et al.*, 2003; Souza *et al.*, 1995). Serine proteinase inhibitors are particularly effective against insects and foraging herbivores and have therefore become a prominent target for use in pest control (Reckel *et al.*, 1997). Legume seeds contain various PIs that have been classified into several families, one of which, the Kunitz-type inhibitors, are one of the best characterized families of plant serine protease inhibitors. In general, Kunitz-type inhibitors are low-molecular-weight proteins of approximately 20 kDa with low cysteine content, resulting in 1–2 intrachain disulfide bonds, and a single reactive site.

The complex of porcine pancreatic trypsin with Kunitz-type soybean trypsin inhibitor (SKTI) has been characterized by X-ray crystallography. Superposition of the complexed (PDB code 1avu) and uncomplexed (PDB code 1avw) forms of SKTI showed obvious changes in the reactive loop and the N-terminal region of the inhibitor, with reduction of the *B* factor upon complex formation (Song & Suh, 1998). In the case of another important protease inhibitor,

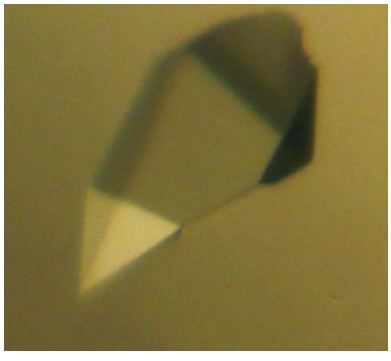

bovine pancreatic trypsin inhibitor (BPTI), the reactive-loop region and C-terminal region were found to coordinate to trypsin (Capasso *et al.*, 1998). This highlights the involvement of different regions of protease inhibitors in interactions with the counterpart proteases, enabling different inhibition mechanisms. The ability of a protease inhibitor to interact with a protease depends on the structural framework of the surface residues of the inhibitor. Some Kunitz-type inhibitors can inhibit a range of proteases, whereas others are protease-specific (He *et al.*, 2008; Milstone *et al.*, 2000). Modelling of the structure of *Erythrina caffra* trypsin inhibitor (ETI) based on SKTI confirmed the role of the surface residues as the main factor in selection of the interacting partner (Song & Suh, 1998). Although a large number of sequences of trypsin inhibitors are available in sequence databases, basic knowledge of the mechanism of their inhibitory action remains elusive. Therefore, determination of three-dimensional structures of Kunitz inhibitor–protease complexes should elucidate the molecular mechanism of Kunitz-type protease inhibitors. The structural and molecular-interaction information provided by these structures could subsequently be employed in the design of potential novel protease inhibitors.

In an attempt to study protease–inhibitor interaction, a Kunitz-type proteinase inhibitor from the seeds of *Tamarindus indica* was cocrystallized with porcine trypsin. Here, we report the crystallization and preliminary X-ray diffraction analysis of this complex of a Kunitz-type proteinase inhibitor with trypsin.

2. Experimental procedure

2.1. Complex formation and purification

Tamarind trypsin inhibitor (TTI) from the seed kernel of *T. indica* was purified according to a previously published protocol (Patil *et al.*, 2009). Porcine pancreatic trypsin was obtained from Sigma–Aldrich. The complex was prepared by mixing 50 µl purified Kunitz-type protease inhibitor at a concentration of 10 mg ml^{-1} in a buffer solution containing 100 m*M* Tris pH 7.4 with 50 µl porcine trypsin at a concentration of 10 mg ml^{-1} in a buffer solution containing 100 m*M* Tris pH 7.4 and 40 m*M* $CaCl_2$. The protease–inhibitor mixture was then incubated at 277 K for 2 h. For purification of the protease–inhibitor complex , 100 µl of the mixture was loaded onto a Superdex-200 GL 10/300 (GE Healthcare) size-exclusion column using a 100 µl sample loop at 0.5 ml min^{-1} on an ÄKTA Purifier FPLC system (GE Healthcare). Elution of the protein was detected by UV absorbance at 280 nm. The size-exclusion column was calibrated with Gel Filtration Calibration LMW standards (GE Healthcare; blue dextran, thyroglobulin, ferritin, aldolase, conalbumin and ovalbumin) for determination of the void volume, construction of the standard curve and estimation of the molecular weight of the complex. The eluted fractions corresponding to the molecular weight of the protease–inhibitor complex were analyzed on 15% reducing SDS–PAGE. The fractions containing the trypsin–TTI complex were pooled and concentrated to 5 mg ml^{-1} at 277 K using an Amicon Ultra-4 10 kDa cutoff concentrator (Millipore). The protein concentration was determined with the Bio-Rad protein-assay kit using bovine serum albumin (BSA) as a standard.

2.2. Crystallization

Crystallization was performed by the sitting-drop method at 293 K using Crystal Screens I and II and Salt Screen (Hampton Research, USA) for initial screening in 96-well crystallization plates (Hampton Research, USA). Drops were prepared by mixing 2 µl protein solution with 2 µl precipitant solution and were equilibrated against 50 µl reservoir solution. Tamarind inhibitor–porcine trypsin complex crystals grew under various conditions, but the best quality crystals grew in 4 *M* ammonium acetate and 0.1 *M* sodium acetate trihydrate pH 4.6.

2.3. Data collection and analysis

Crystals were mounted in cryoloops (Hampton Research, USA) and flash-cooled by direct immersion in liquid nitrogen prior to X-ray diffraction analysis. Data were collected on a MAR 345dtb image-plate system using Cu $K\alpha$ radiation generated by a Bruker Microstar-H rotating-anode generator operated at 45 kV and 60 mA and equipped with Helios optics. Data were collected as 90 images with a crystal-to-detector distance of 170 mm and 1° oscillation per image. The time of exposure was 10 min. The crystal diffracted to 2.0 Å resolution. The diffraction data were processed and scaled with the *AutoMAR* program (Bartels & Klein, 2003).

3. Results and discussion

The Kunitz-type protease inhibitor isolated from the seeds of *T. indica* was found to possess trypsin-inhibitory activity (Patil *et al.*, 2009).

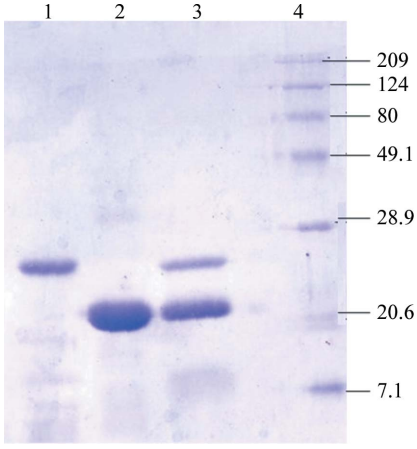

Figure 1
15% SDS–PAGE. Lane 1, porcine trypsin; lane 2, tamarind trypsin inhibitor TTI; lane 3, the major gel-filtration peak fraction containing the complex between TTI and trypsin; lane 4, protein molecular-weight markers (kDa).

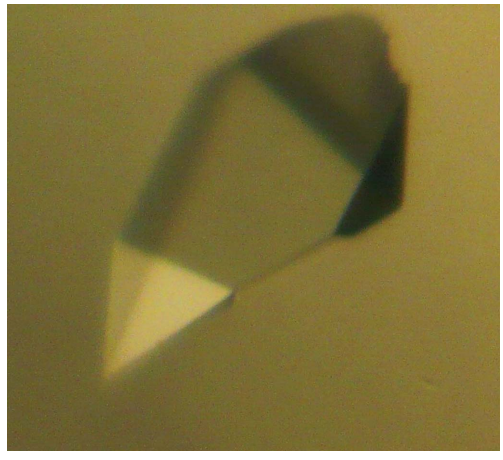

Figure 2
A crystal of the complex between tamarind trypsin inhibitor (TTI) and trypsin. The longest dimension of a typical crystal was between 80 and 100 µm.

Table 1
Data-collection and processing statistics.

Values in parentheses are for the highest resolution shell.

Space group	$P4_1$
Unit-cell parameters (Å, °)	$a = b = 57.1$, $c = 120.1$, $\alpha = \beta = \gamma = 90$
Resolution range	50.0–2.0 (2.1–2.0)
Completeness (%)	94.7 (91.3)
$R_{\rm merge}$† (%)	8.6 (28.4)
Mean $I/\sigma(I)$	6.7 (2.3)
No. of observed reflections	66954
No. of unique reflections	24675 (3198)
Redundancy	2.9 (2.1)
Mosaicity (°)	0.7

† $R_{\rm merge} = \sum_{hkl}\sum_i |I_i(hkl) - \langle I(hkl)\rangle| / \sum_{hkl}\sum_i I_i(hkl)$, where $I_i(hkl)$ is the ith observation of reflection hkl and $\langle I(hkl)\rangle$ is the weighted average intensity for all observations i of reflection hkl.

Therefore, an attempt was made to prepare a protein–protein complex between porcine trypsin and TTI. For complex formation, porcine trypsin and TTI were mixed and the mixture was incubated at 277 K for 2 h. As described above, size-exclusion chromatography was employed to purify the protease–inhibitor complex from the incubated mixture of TTI and trypsin. The molecular weight of the major elution peak from a Superdex-200 GL 10/300 (GE Healthcare) size-exclusion column was calculated using a standard curve and was estimated to be ∼44 kDa, which corresponded to the expected molecular weight of the TTI–trypsin protein complex. Additionally, to confirm the presence of the complex in the major elution peak, peak fractions were run on reducing 15% SDS–PAGE and protein bands corresponding to trypsin (∼23 kDa) and TTI (∼21 kDa) were observed (Fig. 1). The fractions containing the complex were subsequently pooled and concentrated to 15 mg ml^{-1}. The complex crystals of TTI and trypsin were obtained in 20 d at 293 K by vapour diffusion of a 4 µl sitting drop against 50 µl reservoir solution containing 4 *M* ammonium acetate and 0.1 *M* sodium acetate trihydrate pH 4.6 (Fig. 2). Cryoprotection was achieved by the high concentration of ammonium acetate. Diamond-shaped crystals were obtained that belonged to the tetragonal space group $P4_1$ and diffracted to 2.0 Å resolution in-house.

The unit-cell parameters were found to be $a = b = 57.1$, $c = 120.1$ Å, $\alpha = \beta = \gamma = 90°$, with one binary complex of porcine trypsin and tamarind inhibitor per asymmetric unit. This corresponds to a crystal volume per unit molecular weight ($V_{\rm M}$) of 2.26 Å^3 Da^{-1}, given the molecular weight of 44 kDa for the protein complex, with a solvent content of 45% (Matthews, 1968). The data-collection statistics are summarized in Table 1.

The authors are grateful to and thank the Macromolecular Crystallographic Facility (MCU) at IIC, IIT Roorkee for data collection. DNP thanks MHRD, Government of India, MD and ST thank AICTE and Preeti thanks CSIR for financial support.

References

Antão, C. M. & Malcata, F. X. (2005). *Plant Physiol. Biochem.* **43**, 637–650.
Bartels, K. S. & Klein, C. (2003). *The AUTOMAR Manual*, v.1.4. Norderstedt, Germany: MAR Research GmbH.
Capasso, C., Rizzi, M., Menegatti, E., Ascenzi, P. & Bolognesi, M. (1998). *J. Mol. Recognit.* **10**, 26–35.
He, Y. Y., Liu, S. B., Lee, W. H., Qian, J. Q. & Zhang, Y. (2008). *Peptides*, **29**, 1692–1699.
Macedo, M. L. R., Matos, D. G. G., Machado, O. L. T., Marangoni, S. & Novello, J. C. (2000). *Phytochemistry*, **54**, 553–558.
Macedo, M. L. R. & Xavier-Filho, J. (1992). *J. Sci. Food Agric.* **58**, 55–58.
Matthews, B. W. (1968). *J. Mol. Biol.* **33**, 491–497.
Mello, M. O., Tanaka, A. S. & Silva-Filho, M. C. (2003). *Mol. Phylogenet. Evol.* **27**, 103–112.
Milstone, A., Harrison, L., Bungiro, R., Kuzmic, P. & Cappello, M. (2000). *J. Biol. Chem.* **275**, 29391–29399.
Neurath, H. (1984). *Science*, **224**, 350–357.
Neurath, H. (1986). *J. Cell. Biochem.* **32**, 35–49.
Patil, D. N., Preeti, Chaudhry, A., Sharma, A. K., Tomar, S. & Kumar, P. (2009). *Acta Cryst.* F**65**, 736–738.
Reckel, R. K., Kramer, K. J., Baker, J. E., Kanost, M. R., Fabrick, J. A. & Behnke, G. A. (1997). *Advances in Insect Control. The Role of Transgenic Plants*, edited by N. Carozzi & M. Koziel, pp. 157–183. London: Taylor & Francis.
Song, H. K. & Suh, S. W. (1998). *J. Mol. Biol.* **275**, 347–363.
Souza, E. M. T., Mizuta, K., Sampaio, M. U. & Sampaio, C. A. M. (1995). *Phytochemistry*, **39**, 521–525.